NEOPLASMA accepted, ahead of print manuscript
Cite article as https://doi.org/10.4149/neo_2024_230904N469

Running title: DDX46 contributes to pancreatic cancer

Oncogenic DDX46 promotes pancreatic cancer development and gemcitabine resistance by facilitating the JMJD6/CDK4 signaling pathway

Guang Yang, Yun Wang, Kairui Wang, Xinjia Liu, Jing Yang*

Department of Oncology, Tangdu Hospital, Air Force Medical University, Xi'an, Shaanxi, China

*Correspondence: sevenhazel@163.com

Received September 4, 2023 / Accepted May 14, 2024

Pancreatic cancer (PAAD) is a fatal malignancy with a poor prognosis. The treatment strategies are quite limited and gemcitabine is the canonical one, which has been proven to improve the prognosis of PAAD patients. However, the treatment efficiency of gemcitabine is far from satisfactory and remains to be further improved. DEAD-Box Helicase 46 (DDX46) is a kind of RNA helicase, which promotes multiple cancers development. However, its role in PAAD is largely unknown. In the present study, we found DDX46 was highly expressed in PAAD tissues and correlated with poor prognosis. Knockdown of DDX46 repressed PAAD cell growth *in vitro* and *in vivo* and sensitized PAAD cells to gemcitabine treatment. Mechanically, DDX46 bound to JMJD6 and promoted JMJD6/CDK4 signaling pathway. Overexpression of JMJD6 reversed the anti-tumor function of DDX46 knockdown. Our study found a novel pathological mechanism of PAAD progression and provided a potential therapeutic target to improve gemcitabine efficiency.

Key words: pancreatic cancer; DDX46; gemcitabine resistance

Pancreatic cancer (PAAD) is one of the most malignant cancer in the world. Despite the developing scan and test approaches, it's still difficult to diagnose PAAD in the early stage. Most of the patients lose the opportunity to receive surgical resection when they are firstly diagnosed [1]. It's reported the five-year survival rate is around 5-7% [2]. Due to the dismal prognosis, more and more efforts are devoted to exploring the underlying mechanism and potential therapeutic approaches. Accumulating signaling pathways and therapeutic targets have been discovered to uncover the pathological mechanism and aid cancer therapy [3, 4]. Despite these successful developments, it's essential to further explore this issue.

Though immunotherapy, target therapy and radiotherapy have been used to treat PAAD, the benefits acquired from these treatments are quite limited [5, 6]. So far, chemotherapy is still the most commonly used treatment for PAAD patients. Gemcitabine is one of the most effective drugs of chemotherapy [7]. Imported by the human equilibrative nucleoside transporter 1 (hENT1), gemcitabine represses cancer cell proliferation and inhibits cancer development [8]. Compared to a clinical benefit response of 4.8% of 5-FU, single agent gemcitabine achieves a clinical benefit response of 23.8%. Gemcitabine has been recommended as a reference first-line therapy drug for PAAD [9]. However, it's essential to further improve the treatment efficacy of gemcitabine and prolong the prognosis of PAAD patients.

DEAD-Box Helicase 46 (DDX46) is a member of the DEAD box protein family which is a putative RNA helicase [10]. DDX46 participates in modulating translation process, ribosome function and nuclear splicing [11, 12]. DDX46 has been reported to promote multiple cancers development. In gastric cancer, DDX46 enhances the Akt/GSK-3β/β-catenin pathway to promote cancer cell proliferation and invasion [13]. DDX46 also promotes breast cancer, colorectal cancer, osteosarcoma, esophageal squamous cell carcinoma and cutaneous squamous cell carcinoma progression by regulating multiple mechanisms [14-18]. However, the role of DDX46 in PAAD is largely unknown and remains to be fully explored.

Therefore, we aimed to investigate the expression pattern of DDX46 in PAAD. Furthermore, we explored the function of DDX46 in PAAD progression and uncovered the underlying mechanism. We hoped to identify potential targets to improve PAAD prognosis.

Materials and methods

Clinical samples. PAAD tissues and corresponding normal tissues (at least 3 cm from the cancer) were obtained from the PAAD patients who received surgical resection in the Tangdu hospital of Fourth Military Medical University (Xi'an, China). The tissues were immediately preserved in RNAsafer Stabilizer Reagent (R1100, Applygen, Beijing, China) on the ice and transferred to the lab. The tissues were then washed with PBS quickly and stored in liquid nitrogen. The time between tissues collection and their freezing is within about 30 min. The written informed consents were obtained from the patients. All procedures with the human tissue were approved by the Research

Ethics Committee of Tangdu Hospital (202203-106).

Bioinformatic analysis. The DDX46 mRNA expression was analyzed in TCGA PAAD and GTEx pancreas datasets using GEPIA2 online tool (http://gepia2.cancer-pku.cn/#index) [19]. The survival analysis was conducted using the Kaplan-Meier Plotter online tool (http://kmplot.com/analysis/) [20].

Cell culture. The PAAD cell lines MIA-PaCa2 and PANC-1 were obtained from Procell Life Science & Technology Company (Wuhan, China). MIA-PaCa2 cells and PANC-1 cells were both cultured in DMEM medium (PM150210, Peocell, Wuhan, China) supplemented with 10% fetal bovine serum (26010074, Gibco, New York State, USA) and 1% penicillin-streptomycin. A total of 60-70% confluence was suitable for experiments. The cells were infected with lentivirus encoding shRNA to DDX46 or jumonji domain containing 6 (JMJD6). The shRNA sequences for DDX46 were as followes: sh1- DDX46 (5'- CCCATCCAAACCCAAGCTATT-3'); sh2-DDX46 (5'-GCAGAAATCACCAGGCTCATA-3'); sh3-DDX46 (5'-GTGATTGTGATTGAAGAAGAA-3'). The Accession number for JMJD6 overexpression: NM_001081461.2→NP_001074930.1. The Gene ID is 23210, which codes for bifunctional arginine demethylase and lysyl-hydroxylase JMJD6 isoform 1. For selection, 10 μg/ml puromycin was used to eliminate the non-transduced cells.

qRT-PCR. The total mRNA from tumor and corresponding normal tissues were extracted using the total RNA extraction kit (R1200, Solarbio, Beijing, China) according to the protocol provided by the manufacturer. Then the total mRNA was transcribed into complementary DNA. After that, we tested the mRNA expression of DDX46. The reaction was conducted using the RT-qPCR SYBR kit (11143ES50, Yeasen, Shanghai, China) under the following condition: 95 °C for 5 min, 40 cycles of 95 °C for 10 s, and 60 °C for 30 s. $2^{-\Delta\Delta CT}$ method was used to analyzed the target gene expression. According to the MIQE guidelines [21], GAPDH and Actin expression was used as the internal control. The primers sequences were as follows: DDX46, forward: CGGGAGTCACGCCACTATC; reverse: CCTGCTACGAGACCTCTCTCT. GAPDH, forward: ACAACTTTGGTATCGTGGAAGG; reverse: GCCATCACGCCACAGTTTC. Actin, forward: GGCATTCACGAGACCACCTAC; reverse: CGACATGACGTTGTTGGCATAC.

Western blot. The lysis buffer (P0013C, Beyotime, Shanghai, China) was used to extract the protein from PAAD/normal tissues and PAAD cell lines. The tissues and cells were incubated with

lysis buffer in the ice for 30 min with frequent shaking. Then the samples were centrifuged at 14,000 × g for 12 min. The supernatant was collected and used to examine the protein concentration using BCA protein assay kit (23225, Thermo, MA, US). Next, we diluted the samples to the same concentration. A total of 20 μg protein samples/lane were separated in SDS-page. After that, the proteins were transferred to the polyvinylidene fluoride membranes. Then the membranes were blocked with 5% non-fat milk and incubated with primary antibodies overnight at 4 °C. DDX46 primary antibody (16927-1-AP, Proteintech, Wuhan, China), JMJD6 primary antibody (sc-28348, Santa Cruz, US), CDK4 primary antibody (11026-1-AP, Proteintech), GAPDH primary antibody (AC033, Abclonal, Wuhan, China), Actin primary antibody (A1011, Abclonal) and Tubulin primary antibody (AC012, Abclonal) were used as manufacturers suggested. After that membrane was washed three times with TBST for 5 min and incubated with HRP goat anti-rabbit IgG antibody (AS014, Abclonal) or HRP goat anti-mouse IgG (AS003, Abclonal) for 2 h at room temperature. Bio-Rad ChemiDocXRS+ (170-8265, Bio-Rad, California, USA) was used to detect the protein expression.

Immunohistochemistry (IHC). The PAAD and corresponding normal tissues and mice PAAD model tissues were fixed in 4% paraformaldehyde. Xylene was used to eliminate the paraffin in tissue sections. After that, ethanol was used to rehydrate these sections. 3% hydrogen was used to inhibit the peroxide activity and 10% normal serum was used to block the sections. Then the sections were incubated with DDX46 and Ki67 primary antibodies (27309-1-AP, Proteintech) overnight at 4 °C. The sections were incubated with secondary antibodies for 2 h and with hematoxylin for 5 min.

Cell counting kit8 (CCK8). The MIA-PaCa2 and PANC-1 cells were seeded in 96 wells plate for 24 h. Sterilized water was used to dissolve the gemcitabine into a 30 mM solution. Then the cells were treated with gemcitabine with indicated concentrations for 24 h. The cells in control group were treated with the same volume of sterilized water. After that, the medium was removed and PBS was used to wash cells gently three times. CCK8 reagent was added to the culture medium and the diluted working buffer was added to each well. After incubating for 1.5 h, the absorbance was measured at 450 nm.

Cell cycle analysis. 1×10^6 MIA-PaCa2 and PANC-1 cells were seeded in 6-wells plates for 24 h.

Trypsin was used to digest cells and PBS was used to resuspend the cells. After that, the cells were fixed with precooled 70% ethanol for at least 6 h at 4 °C. Then the cells were stained with PI/RNase staining buffer (550825, BD, US) for 15 min and subjected to flow cytometry analysis (FACS Calibur, BD, USA).

EdU (5-Ethynyl-2'- deoxyuridine) staining. EdU staining was used to analyze the cell proliferation rate. Similar to cell cycle analysis, cells were cultured for 24 h and washed with PBS three times. Then cells were incubated with EdU working buffer (10μM) for 1h (C0071, Beyotime, Shanghai, China). After that, the medium was removed and cells were washed with PBS three times and fixed with 4% paraformaldehyde for 15 min. Then cells were permeabilized with 0.3% Triton-X100 for 15 min and incubated with Click Additive Solution for 30 min in dark. Finally, cells were stained with DAPI for 15 min to label the nuclear. Cells were observed with confocal microscope (A1, Nikon, Japan).

Cell apoptosis assay. Similar to CCK8 assay, cells were treated with gemcitabine for 24 h at indicated concentration. Then cells were digested with trypsin without EDTA. After that, cells were stained with Annexin-V and PI buffer for 15 min (556507, BD, US). The apoptosis rate was analyzed using the flow cytometry analysis (FACS Calibur, BD, USA).

Co-immunoprecipitation. The MIA-PaCa2 cells were washed with PBS for three times and digested with trypsin. Then gentle lysis buffer (P0013, Beyotime, Shanghai, China) was used to extract protein. The cells were incubated in the ice for 1 h with constant shaking. After that, cells were centrifuged at the speed of 14000 RCF and the supernatant was collected and treated with RNase A (100 mg/ml) and Dnase - (2,000 U/ml) for 1 h. Primary antibodies or control IgG antibody was added to the supernatant overnight at 4 °C. Then the magnetic beads binding to protein A/G (B23201, Bimake, Texas, USA) was washed three times with lysis buffer and was added to the supernatant for another 6 h. After that, the magnetic beads were enriched and washed three times with lysis buffer for 5 min each time. Finally, the protein expression was analyzed as suggested in western blot section.

Immunofluorescence. When MIA-PaCa2 cells were seeded on the slides for 24 h, washed the cells with PBS and fixed them using the 4% paraformaldehyde for 15 min. Penetrate the cells with 0.3% Triton-X100 buffer for 15 min and blocked the cells with 3% BSA for 15 min. Then incubated cells

with primary DDX46 and JMJD6 antibodies overnight at 4 °C. Cells were washed with PBS and then incubated the cells with goat anti-mouse IgG (H+L) Alexa Fluor™ 488 secondary antibody (A-11001, Thermo, US) and goat anti-rabbit IgG (H+L) Alexa Fluor™ Plus 647 secondary antibody (A32733, Thermo) for 2 h at room temperature in dark. Finally, cells were stained with DAPI for 10 min to label the nuclei. The protein location was observed with confocal microscope (A1, Nikon, Japan).

Animal studies. The 8-weeks old male BALB/c nude mice were purchased from the animal center of Fourth Military Medical University and kept in SPF environment. When MIA-PaCa2 cells were 80% confluent, control and DDX46 knockdown cells were harvested and counted. 2×10^6 MIA-PaCa2 cells were resuspended with 150 µl PBS and injected subcutaneously into nude mice (n=5). The tumors were measured every three days. The volume was calculated using the formula (volume=longest diameter × shortest diameter^2 × 0.5). The mice were euthanized with carbon dioxide and tumors were resected. All procedures involving the animal study were approved by the Research Ethics Committee of Tangdu Hospital (TDLL2018-03-104).

Statistical analysis. The experimental data were analyzed with SPSS 20.0. The experiment data were all represented as a mean estimate±standard deviation of at least three independent replicates. Student's t-test was used to analyzed the data acquired from two groups. Analysis of variance was used to analyzed the data derived from three or more groups. P-values (*$p < 0.05$, **$p < 0.01$, and ***$p < 0.001$) were suggested as statistically significant.

Results

DDX46 was highly expressed in PAAD and correlated with poor prognosis of PAAD patients. To explore the expression pattern of DDX46 in cancers, we analyzed the TCGA datasets by using the GEPIA2 online tool. The result showed that DDX46 was highly expressed in many kinds of cancers including PAAD, breast invasive carcinoma, colon adenocarcinoma, esophageal carcinoma, acute myeloid leukemia, stomach adenocarcinoma and others (Figures 1A, 1B). To further validate the result, we analyzed the mRNA and protein expression of DDX46 in PAAD and corresponding tissue we collected. The qRT-PCR results indicated DDX46 mRNA was highly expressed in PAAD tissues compared with normal tissues (Figure 1C). The western blot and IHC result both suggested

that DDX46 protein was increased in PAAD tissues, which was consistent with the mRNA result (Figures 1D, 1E). Next, we explore the relationship between DDX46 expression with prognosis of PAAD patients. The result suggested that high expression of DDX46 was related with poor overall survival and relapse-free survival despite the fact that they were not statistically significant (Supplementary Figures S1A, S1B). These results hinted that DDX46 might be involved in PAAD progression.

DDX46 knockdown repressed PAAD cell proliferation. To explore the effect of DDX46 on PAAD development, we knocked down DDX46 in MIA-PaCa2 and PANC-1 cells by transducing them with lentivirus encoding shRNA for DDX46. The results showed that DDX46 was successfully decreased in sh#1 and sh#2 groups when compared with negative control group (Figures 2A, 2B). The cell counting results suggested that DDX46 knockdown significantly decreased the cell proliferation when compared with control group in in MIA-PaCa2 and PANC-1 cells (Figures 2C, 2D). Next, we analyzed the cell cycle of DDX46 knockdown and control cells. The results confirmed that the percentage of cells in S phase greatly decreased in DDX46 knockdown cells (Figures 2E, 2F). To further validate the result, EdU assay was conducted to assess the proliferation rate of DDX46 knockdown cells. The results indicated proliferation rate of DDX46 knockdown cells was decreased, which was consistent with cell counting and cell cycle results (Figures 2G, 2H). The present results hinted that DDX46 knockdown inhibited PAAD cell proliferation.

DDX46 knockdown sensitized PAAD cells to gemcitabine. Gemcitabine is one of the most commonly used and potent drugs for treating PAAD. We tried to examine whether DDX46 affected PAAD cell response to gemcitabine. Firstly, we treat MIA-PaCa2 and PANC-1 cells with different concentrations of gemcitabine for 24 h. The result showed that gemcitabine induced cell death in a dose-dependent manner and 100 and 150 nM gemcitabine induced almost 50% cell death rate of MIA-PaCa2 and PANC-1 cells respectively (Figures 3A, 3B). 100 and 150 nM gemcitabine were used to treat MIA-PaCa2 and PANC-1 cells respectively in later experiments. The result showed that the cell viability of DDX46 knockdown cells significantly decreased after gemcitabine treatment when compared with control cells treated with gemcitabine (Figures 3C, 3D). We also examined the apoptosis rate of DDX46 knockdown cells treated with gemcitabine. The result

indicated that the apoptosis rate of DDX46 knockdown cells greatly increased when compared with control cells treated with gemcitabine (Figures 3E, 3F). These results demonstrated that DDX46 knockdown made PAAD cells more sensitive to gemcitabine treatment.

DDX46 regulated JMJD6/CDK4 signaling pathway in PAAD cell. To explore the underlying mechanism accounting for DDX46 function, we searched for DDX46 targets using HitPredict tool (http://www.hitpredict.org/). The result suggested JMJD6 was the potential target gene for DDX46 (Data was not shown). We verified this result using the co-immunoprecipitation assay. The result proved that DDX46 directly bound to JMJD6 in MIA-PaCa2 cells (Figures 4A, 4B). The confocal result also confirmed that DDX46 and JMJD6 co-localized in cell nuclei (Figure 4C). To further test the effect of DDX46 on JMJD6, we examined JMJD6 and its target gene CDK4 expressions in DDX46 knockdown cells. The result indicated that DDX46 knockdown decreased JMJD6 and CDK4 protein expressions when compared with control MIA-PaCa2 cells (Figures 5A-5C) and PANC-1 cells (Figures 5D-5F). The results proved that DDX46 positively modulated JMJD/CDK4 signaling pathway.

Overexpression of JMJD6 reversed the effect of DDX46 knockdown on PAAD cell proliferation and sensitivity to gemcitabine. To further confirm DDX46 knockdown affected PAAD development by regulating JMJD6/CDK4 signaling pathway. The JMJD6 overexpression vector was constructed (Supplementary Figure S2). we then overexpressed JMJD6 in DDX46 knockdown MIA-PaCa2 (Figure 6A) and PANC-1 cells (Figure 6B). The cell counting results showed that DDX46 knockdown decreased cell viability when compared with control cells, while overexpression of JMJD6 reversed the inhibitory effect of DDX46 knockdown on cell viability when compared with DDX46 knockdown cells (Figures 6C, 6D). Furthermore, we found that overexpression of JMJD6 decreased the apoptosis rate of PAAD cell treated with gemcitabine when compared with DDX46 knockdown cells (Figure 6E). These results indicated DDX46 knockdown affected PAAD cell proliferation and sensitivity to gemcitabine by restraining JMJD6/CDK4 signaling pathway.

DDX46 knockdown suppressed PAAD growth in mice. To explore the effect of DDX46 on PAAD development *in vivo*, we constructed the PAAD subcutaneous model in nude mice. The result confirmed that DDX46 knockdown curbed the tumor growth in nude mice (Figure 7A). Detailly, the volume and weight of DDX46 knockdown tumors both decreased when compared with the control tumors (Figures 7B, 7C). We also analyzed the Ki67 expression in tumors. The result showed that Ki67 was decreased in DDX46 knockdown tumors when compared with control tumors (Figure 7D). The above results proved that DDX46 knockdown constricted tumor growth *in vivo*.

Discussion

PAAD is a kind of malignant tumor with poor prognosis. Despite the great development in PAAD treatment, gemcitabine is still one of the most potent drugs that suppresses tumor progression and improves patients' prognosis [22]. Though great progress has been achieved in understanding how PAAD develops, it's essential to further uncover the pathological mechanism and discover potential targets to improve treatment efficiency [3]. In the present study, we found DDX46 exerted a cancer-promoting function in PAAD. DDX46 was highly expressed and associated with poor prognosis of PAAD patients. DDX46 knockdown curbed tumor proliferation and sensitized PAAD

cells to gemcitabine. Mechanically, DDX46 promoted JMJD6/CDK4 signaling pathway to promote PAAD development. Our study revealed a novel mechanism promoting PAAD development and identified DDX46 as a potential target to modulate gemcitabine efficiency.

DDX46 has been found to exert tumorigenic role in many kinds of tumors. By regulating MAPK-p38 signaling, Akt/GSK-3β/β-catenin pathway, autophagy and other pathways, DDX46 promotes cancer cell proliferation and invasion [13]. However, the role of DDX46 is largely unknown in PAAD development. In the present study, we found that DDX46 was highly expressed in PAAD tissues compared with normal tissue. More importantly, DDX46 knockdown suppressed PAAD cell proliferation *in vitro* and *in vivo*. These results proved that DDX46 played a tumorigenic role in PAAD, which was consistent with the results in other tumors.

Gemcitabine has been proved to greatly improve the prognosis of PAAD patients. However, the outcome is still far from our satisfaction and better strategy are urgently needed to further improve gemcitabine efficiency. It has been reported many factors affecting gemcitabine sensitivity of PAAD cells. For example, Ginsenoside Rg3, one of the critical active components of Ginseng, sensitized PAAD cells to gemcitabine [23]. In another research, monocarboxylate transporter 4 (MCT4) is highly expressed in PAAD tissues. Inhibition of MCT4 has a synergistic role with gemcitabine treatment [24]. More and more regulatory factors are being discovered including AK4P1 and DCLK1-AL [25, 26]. Our present study found that DDX46 modulated sensitivity of PAAD cells to gemcitabine. Once DDX46 was silenced, the apoptosis rate of PAAD cells was greatly increased after gemcitabine treatment. Our study provided a novel therapeutic target to improve gemcitabine efficiency.

JMJD6 is a nuclear protein which works as protein hydroxylase or histone demethylase [27]. It has been reported JMJD6 promotes hepatocellular carcinoma development by facilitating CDK4 expression [28]. Also, JMJD6 has been reported to promote prostate cancer, breast cancer, clear cell renal cell carcinoma and many other cancers development [29-31]. However, little is known about JMJD6 in PAAD. Our present study showed that JMJD6 was the downstream target of DDX46. DDX46 directly bound to JMJD6 and promoted JMJD6 expression. Moreover, DDX46 also increased the JMJD6 target gene CDK4 expression. It has been revealed CDK4 was involved in the pathogenesis of PAAD [32, 33]. Our study uncovered a novel pathological mechanism promoting

PAAD progression.

However, there are also some questions remained to be answered. Our study showed that DDX46 and JMJD6 co-localized in nuclear and bound to each other. Moreover, DDX46 promoted JMJD6 protein expression. However, DDX46 is often considered as an RNA helicase, which mainly regulates target gene mRNA expression. Our result seems contradictory to previous result. JMJD6 is a kind of histone demethylase. By binding to and modifying histone modification of CDK4 promoter, JMJD6 promotes CDK4 mRNA expression [28]. For DDX46 and JMJD6 both regulates RNA homeostasis, we deduced that they form a complex to realize RNA-regulation function. Additionally, DDX46 knockdown decreased JMJD6 protein expression. However, the underlying mechanism for JMJD6 degradation is unknown. It's well acknowledged that autophagy and ubiquitin-proteasome system are the most common mechanisms for protein degradation [34]. However, it remains to be explored which one or other mechanisms accounting the JMJD6 degradation.

In conclusion, we found DDX46 was highly expressed in PAAD. DDX46 knockdown decreased PAAD cell proliferation *in vitro* and *in vivo* and exerted a synergistic role with gemcitabine treatment by regulating JMJD6/CDK4 signaling pathway. Our result uncovered a novel mechanism underlying PAAD development and provided a potential therapeutic target to improve gemcitabine efficiency.

Acknowledgements: This work was supported by the Key Research and Development Projects of Shaanxi Province (2022ZDLSF03-01).

Supplementary data are available in the online version of the paper.

References

[1] KLEIN AP. Pancreatic cancer epidemiology: understanding the role of lifestyle and inherited risk factors. Nat Rev Gastroenterol Hepatol 2021; 18: 493-502. https://doi.org/10.1038/s41575-021-00457-x

[2] CAI J, CHEN H, LU M, ZHANG Y, LU B et al. Advances in the epidemiology of pancreatic cancer: Trends, risk factors, screening, and prognosis. Cancer Lett 2021; 520: 1-11. https://doi.org/10.1016/j.canlet.2021.06.027

[3] WOOD LD, CANTO MI, JAFFEE EM, SIMEONE DM. Pancreatic Cancer: Pathogenesis, Screening, Diagnosis, and Treatment. Gastroenterology 2022; 163: 386-402.e1. https://doi.org/10.1053/j.gastro.2022.03.056

[4] KOTSILITI E. Microbial signatures in pancreatic cancer. Nat Rev Gastroenterol Hepatol 2022; 19: 350. https://doi.org/10.1038/s41575-022-00625-7

[5] PADRÓN LJ, MAURER DM, O'HARA MH, O'REILLY EM, WOLFF RA et al. Sotigalimab and/or nivolumab with chemotherapy in first-line metastatic pancreatic cancer: clinical and immunologic analyses from the randomized phase 2 PRINCE trial. Nat Med 2022; 28: 1167-1177. https://doi.org/10.1038/s41591-022-01829-9

[6] MOORE MJ, GOLDSTEIN D, HAMM J, FIGER A, HECHT JR et al. Erlotinib plus gemcitabine compared with gemcitabine alone in patients with advanced pancreatic cancer: a phase III trial of the National Cancer Institute of Canada Clinical Trials Group. J Clin Oncol 2007; 25: 1960-1966. https://doi.org/10.1200/JCO.2006.07.9525

[7] BURRIS HA, MOORE MJ, ANDERSEN J, GREEN MR, ROTHENBERG ML et al. Improvements in survival and clinical benefit with gemcitabine as first-line therapy for patients with advanced pancreas cancer: a randomized trial. J Clin Oncol 1997; 15: 2403-2413. https://doi.org/10.1200/JCO.1997.15.6.2403

[8] NORDH S, ANSARI D, ANDERSSON R. hENT1 expression is predictive of gemcitabine outcome in pancreatic cancer: a systematic review. World J Gastroenterol 2014; 20: 8482-8490. https://doi.org/10.3748/wjg.v20.i26.8482

[9] SINGH RR, O'REILLY EM. New Treatment Strategies for Metastatic Pancreatic Ductal Adenocarcinoma. Drugs 2020; 80: 647-669. https://doi.org/10.1007/s40265-020-01304-0

[10] ULLAH R, LI J, FANG P, XIAO S, FANG L. DEAD/H-box helicases:Anti-viral and pro-viral roles during infections. Virus Res 2022; 309: 198658. https://doi.org/10.1016/j.virusres.2021.198658

[11] ZHENG Q, HOU J, ZHOU Y, LI Z, CAO X. The RNA helicase DDX46 inhibits innate immunity by entrapping m6A-demethylated antiviral transcripts in the nucleus. Nat Immunol 2017; 18: 1094-1103. https://doi.org/10.1038/ni.3830

[12] WILL CL, URLAUB H, ACHSEL T, GENTZEL M, WILM M et al. Characterization of novel SF3b and 17S U2 snRNP proteins, including a human Prp5p homologue and an SF3b DEAD-box protein. EMBO J 2002; 21: 4978-4988. https://doi.org/10.1093/emboj/cdf480

[13] CHEN L, XU M, ZHONG W, HU Y, WANG G. Knockdown of DDX46 suppresses the proliferation and invasion of gastric cancer through inactivating Akt/GSK-3β/β-catenin pathway. Exp Cell Res 2021; 399: 112448. https://doi.org/10.1016/j.yexcr.2020.112448

[14] MA Z, SONG J, HUA Y, WANG Y, CAO W et al. The role of DDX46 in breast cancer proliferation and invasiveness: A potential therapeutic target. Cell Biol Int 2023; 47: 283-291. https://doi.org/10.1002/cbin.11930

[15] LI M, MA Y, HUANG P, DU A, YANG X et al. Lentiviral DDX46 knockdown inhibits growth and induces apoptosis in human colorectal cancer cells. Gene 2015; 560: 237-244. https://doi.org/10.1016/j.gene.2015.02.020

[16] JIANG F, ZHANG D, LI G, WANG X. Knockdown of DDX46 Inhibits the Invasion and Tumorigenesis in Osteosarcoma Cells. Oncol Res 2017; 25: 417-425. https://doi.org/10.3727/096504016X14747253292210
[17] LIN Q, JIN HJ, ZHANG D, GAO L. DDX46 silencing inhibits cell proliferation by activating apoptosis and autophagy in cutaneous squamous cell carcinoma. Mol Med Rep 2020; 22: 4236-4242. https://doi.org/10.3892/mmr.2020.11509
[18] LI B, LI YM, HE WT, CHEN H, ZHU HW et al. Knockdown of DDX46 inhibits proliferation and induces apoptosis in esophageal squamous cell carcinoma cells. Oncol Rep 2016; 36: 223-230. https://doi.org/10.3892/or.2016.4803
[19] TANG Z, KANG B, LI C, CHEN T, ZHANG Z. GEPIA2: an enhanced web server for large-scale expression profiling and interactive analysis. Nucleic Acids Res 2019; 47: W556-W560. https://doi.org/10.1093/nar/gkz430
[20] LÁNCZKY A, GYŐRFFY B. Web-Based Survival Analysis Tool Tailored for Medical Research (KMplot): Development and Implementation. J Med Internet Res 2021; 23: e27633. https://doi.org/10.2196/27633
[21] BUSTIN SA, BENES V, GARSON JA, HELLEMANS J, HUGGETT J et al. The MIQE Guidelines: Minimum Information for Publication of Quantitative Real-Time PCR Experiments. Clinical Chemistry 2009; 55: 611-622. https://doi.org/10.1373/clinchem.2008.112797
[22] MANIAM G, MAI CW, ZULKEFELI M, FU JY. Co-encapsulation of gemcitabine and tocotrienols in nanovesicles enhanced efficacy in pancreatic cancer. Nanomedicine (Lond) 2021; 16: 373-389. https://doi.org/10.2217/nnm-2020-0374
[23] PAN H, YANG L, BAI H, LUO J, DENG Y. Ginsenoside Rg3 increases gemcitabine sensitivity of pancreatic adenocarcinoma via reducing ZFP91 mediated TSPYL2 destabilization. J Ginseng Res 2022; 46: 636-645. https://doi.org/10.1016/j.jgr.2021.08.004
[24] LEE SH, HWANG HK, LEE WJ, KANG CM. MCT4 as a potential therapeutic target to augment gemcitabine chemosensitivity in resected pancreatic cancer. Cell Oncol (Dordr) 2021; 44: 1363-1371. https://doi.org/10.1007/s13402-021-00643-8
[25] QU D, WEYGANT N, YAO J, CHANDRAKESAN P, BERRY WL et al. Overexpression of DCLK1-AL Increases Tumor Cell Invasion, Drug Resistance, and KRAS Activation and Can Be Targeted to Inhibit Tumorigenesis in Pancreatic Cancer. J Oncol 2019; 2019: 6402925. https://doi.org/10.1155/2019/6402925
[26] LI L, DENG T, ZHANG Q, YANG Y, LIU Y et al. AK4P1 is a cancer-promoting pseudogene in pancreatic adenocarcinoma cells whose transcripts can be transmitted by exosomes. Oncol Lett 2022; 23: 163. https://doi.org/10.3892/ol.2022.13283
[27] KWOK J, O'SHEA M, HUME DA, LENGELING A. Jmjd6, a JmjC Dioxygenase with Many Interaction Partners and Pleiotropic Functions. Front Genet 2017; 8: 32. https://doi.org/10.3389/fgene.2017.00032
[28] WAN J, LIU H, YANG L, MA L, LIU J et al. JMJD6 promotes hepatocellular carcinoma carcinogenesis by targeting CDK4. Int J Cancer 2019; 144: 2489-2500. https://doi.org/10.1002/ijc.31816
[29] PASCHALIS A, WELTI J, NEEB AJ, YUAN W, FIGUEIREDO I et al. JMJD6 Is a Druggable Oxygenase That Regulates AR-V7 Expression in Prostate Cancer. Cancer Res 2021; 81: 1087-1100. https://doi.org/10.1158/0008-5472.CAN-20-1807

[30] BISWAS A, MUKHERJEE G, KONDAIAH P, DESAI KV. Both EZH2 and JMJD6 regulate cell cycle genes in breast cancer. BMC Cancer 2020; 20: 1159. https://doi.org/10.1186/s12885-020-07531-8

[31] ZHOU J, SIMON JM, LIAO C, ZHANG C, HU L et al. An oncogenic JMJD6-DGAT1 axis tunes the epigenetic regulation of lipid droplet formation in clear cell renal cell carcinoma. Mol Cell 2022; 82: 3030-3044.e8. https://doi.org/10.1016/j.molcel.2022.06.003

[32] JIGGENS E, MORTOGLOU M, GRANT GH, UYSAL-ONGANER P. The Role of CDK4 in the Pathogenesis of Pancreatic Cancer. Healthcare (Basel) 2021; 9: 1478. https://doi.org/10.3390/healthcare9111478

[33] SALVADOR-BARBERO B, ALVAREZ-FERNÁNDEZ M, ZAPATERO-SOLANA E, EL BAKKALI A, MENÉNDEZ MDC et al. CDK4/6 Inhibitors Impair Recovery from Cytotoxic Chemotherapy in Pancreatic Adenocarcinoma. Cancer Cell 2020; 38: 584. https://doi.org/10.1016/j.ccell.2020.09.012

[34] WANG Y, LE WD. Autophagy and Ubiquitin-Proteasome System. Adv Exp Med Biol2019; 1206: 527-550. https://doi.org/10.1007/978-981-15-0602-4_25

Figure Legends

Figure 1. DDX46 was highly expressed in PAAD and correlated with poor prognosis of PAAD patients. A) The DDX46 mRNA expression in multiple cancer datasets from TCGA. B) The DDX46 mRNA expression in PAAD dataset from TCGA and pancreas dataset from GTEx. C) The DDX46 mRNA expression in PAAD and normal tissues. D) The western blot result of DDX46 protein expression in PAAD and normal tissues. E) The IHC result of DDX46 protein expression in PAAD and normal tissues. $*p < 0.05$, $***p < 0.001$

Figure 2. DDX46 knockdown repressed PAAD cell proliferation. A, B) The western blot results confirmed DDX46 knockdown efficiency in MIA-PaCa2 and PANC-1 cells. C, D) The cell counting result of DDX46 knockdown and control MIA-PaCa2 and PANC-1 cells. E, F) The cell cycle result of DDX46 knockdown and control MIA-PaCa2 and PANC-1 cells. G, H) The EdU result of DDX46 knockdown and control MIA-PaCa2 and PANC-1 cells. $*p < 0.05$, $**p < 0.01$

Figure 3. DDX46 knockdown sensitized PAAD cells to gemcitabine. A, B) The CCK8 assay result of control MIA-PaCa2 and PANC-1 cells treated with different concentrations of gemcitabine. C, D) The CCK8 assay result of DDX46 knockdown and control MIA-PaCa2 and PANC-1 cells treated

with gemcitabine for 24 hours. E) The apoptosis rate of DDX46 knockdown and control MIA-PaCa2 and PANC-1 cells treated with gemcitabine for 24 h. *p < 0.05, **p < 0.01, ***p < 0.001

Figure 4. DDX46 directly bound to JMJD6. A, B) Endogenous binding of DDX46 and JMJD6 was detected using co-IP and western blot assays. C) The confocal result of DDX46 and JMJD6 localization.

Figure 5. DDX46 regulated JMJD6/CDK4 signaling pathway in PAAD cell. A-C) The western blot result of MIA-PaCa2 cells when DDX46 was silenced. D-F) The western blot result of PANC-1 cells when DDX46 was silenced. **p < 0.01, ***p < 0.001

Figure 6. Overexpression of JMJD6 reversed the effect of DDX46 knockdown on PAAD cell proliferation and sensitivity to gemcitabine. A, B) The western blot result of MIA-PaCa2 and PANC-1 cells when DDX46 was silenced with or without JMJD6 overexpression. C, D) The cell counting result of MIA-PaCa2 and PANC-1 cells when DDX46 was silenced with or without JMJD6 overexpression. E) The apoptosis rate of MIA-PaCa2 and PANC-1 cells when DDX46 was silenced with or without JMJD6 overexpression. ns represents p > 0.05, *p < 0.05, **p < 0.01, ***p < 0.001

Figure 7. DDX46 knockdown suppressed PAAD growth in mice. A) The xenografts from DDX46 knockdown and control MIA-PaCa2 cells in nude mice. B) The volume of xenografts from DDX46 knockdown and control MIA-PaCa2 cells in nude mice. C) The weight of xenografts from DDX46 knockdown and control MIA-PaCa2 cells in nude mice. D) The IHC result of Ki67 staining in xenografts from DDX46 knockdown and control MIA-PaCa2 cells. *p < 0.05, **p < 0.01, ***p < 0.001

Fig. 1 [Download full resolution image]

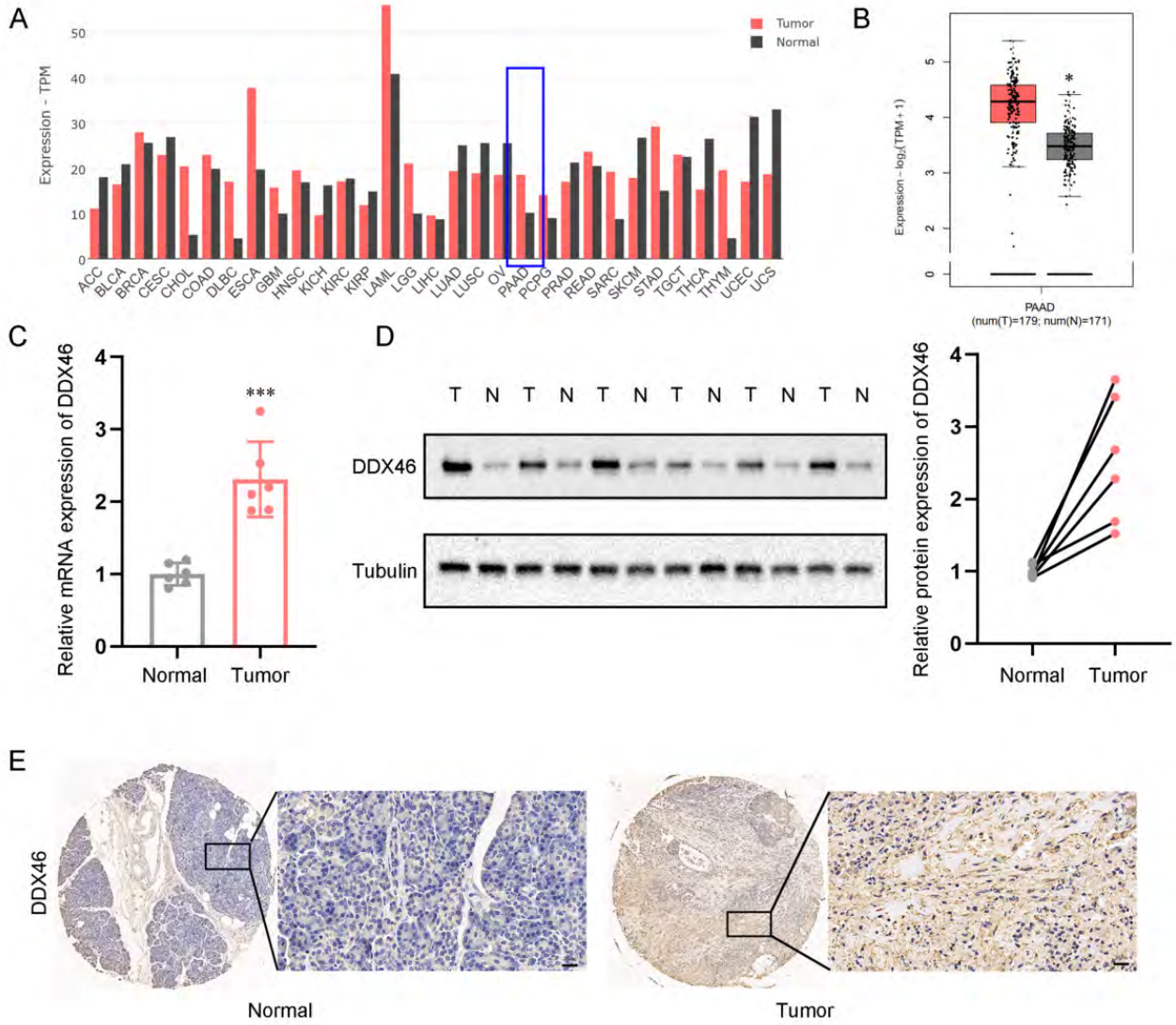

Fig. 2 [Download full resolution image]

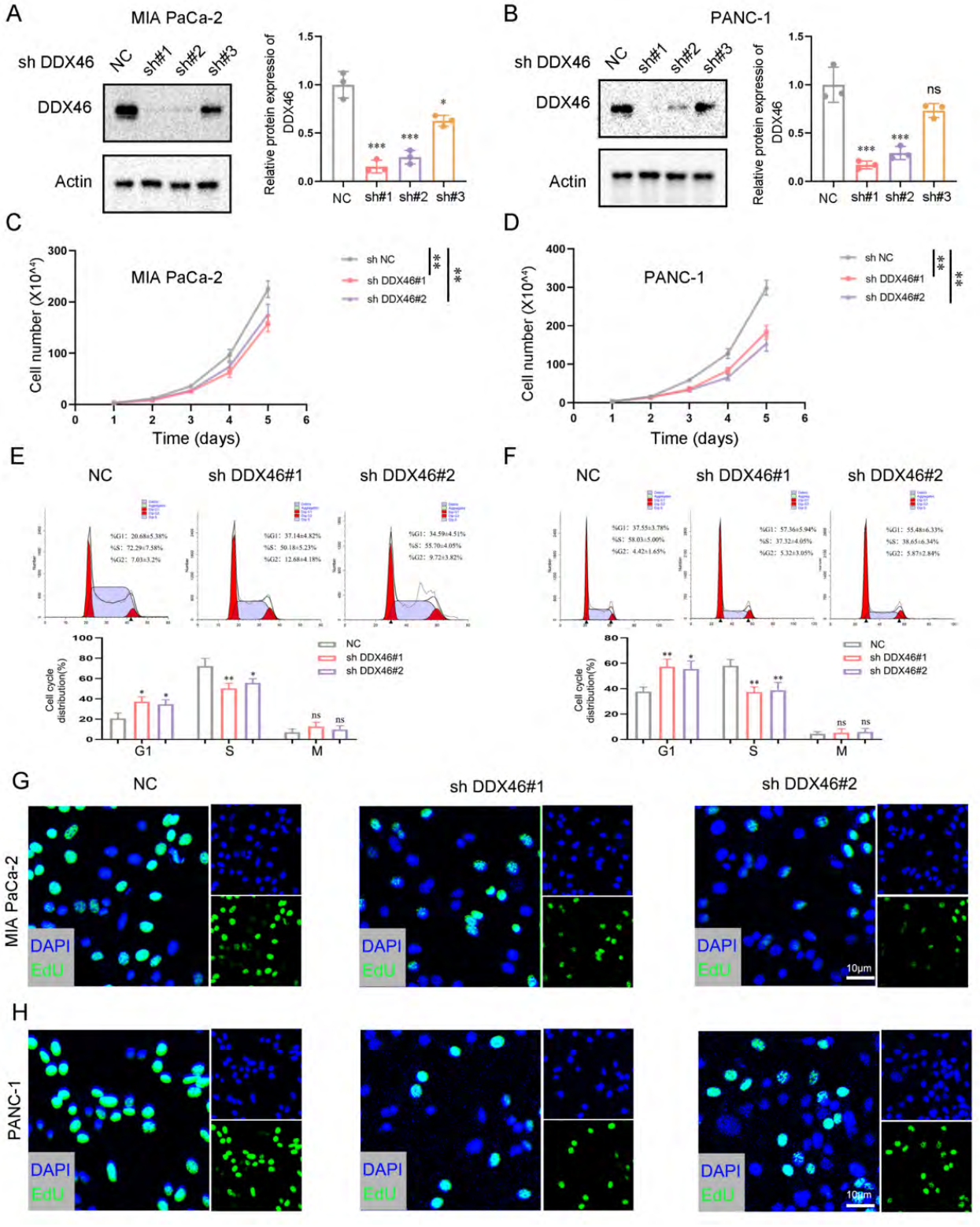

Fig. 3 Download full resolution image

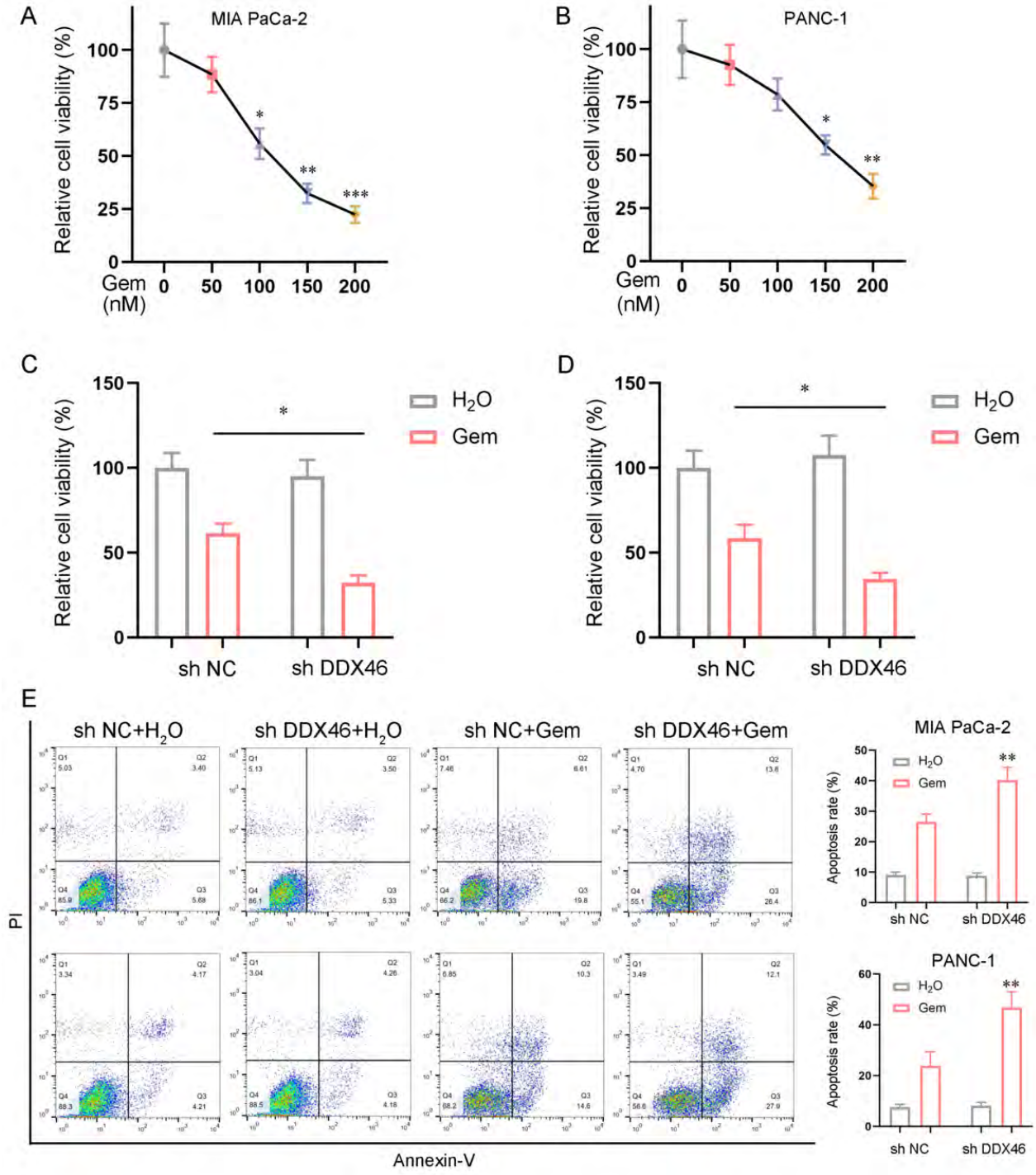

Fig. 4 Download full resolution image

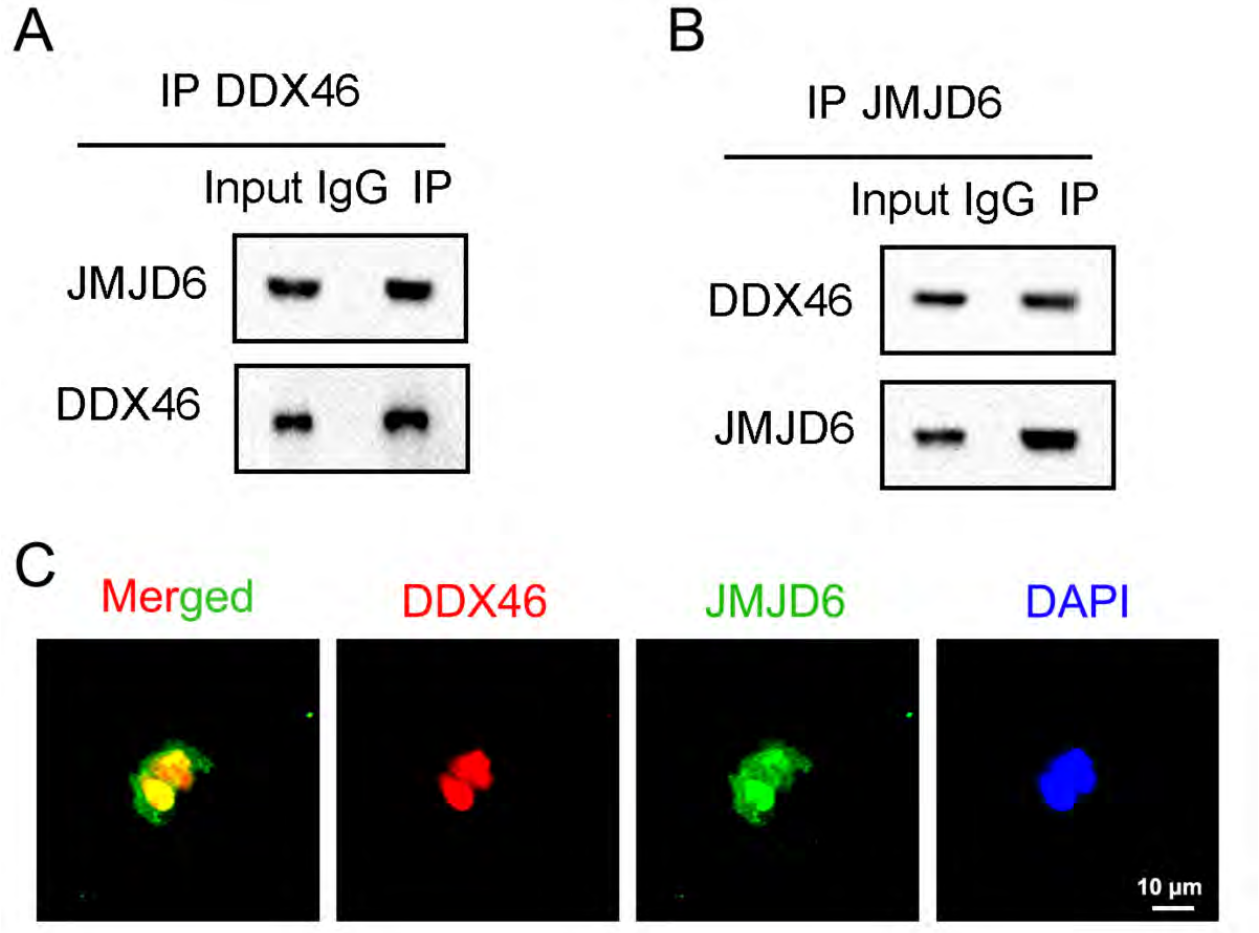

Fig. 5 Download full resolution image

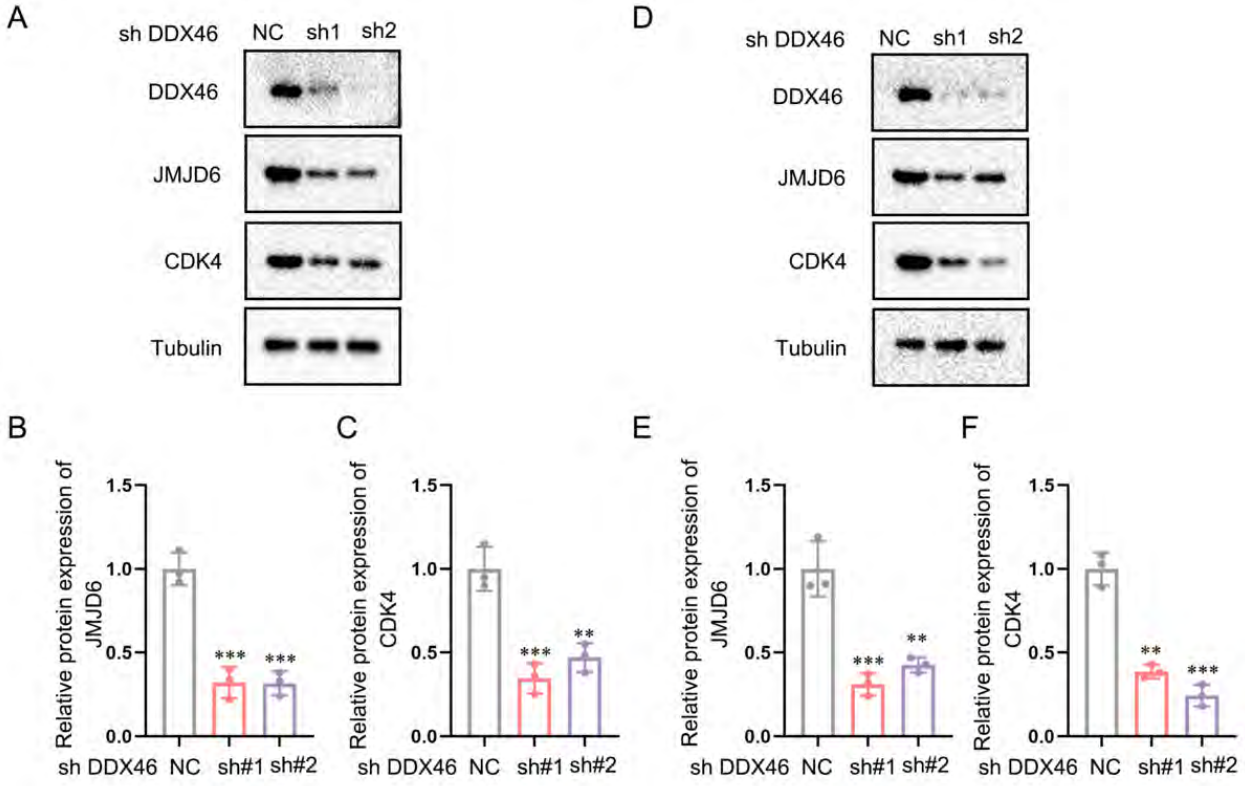

Fig. 6 [Download full resolution image]

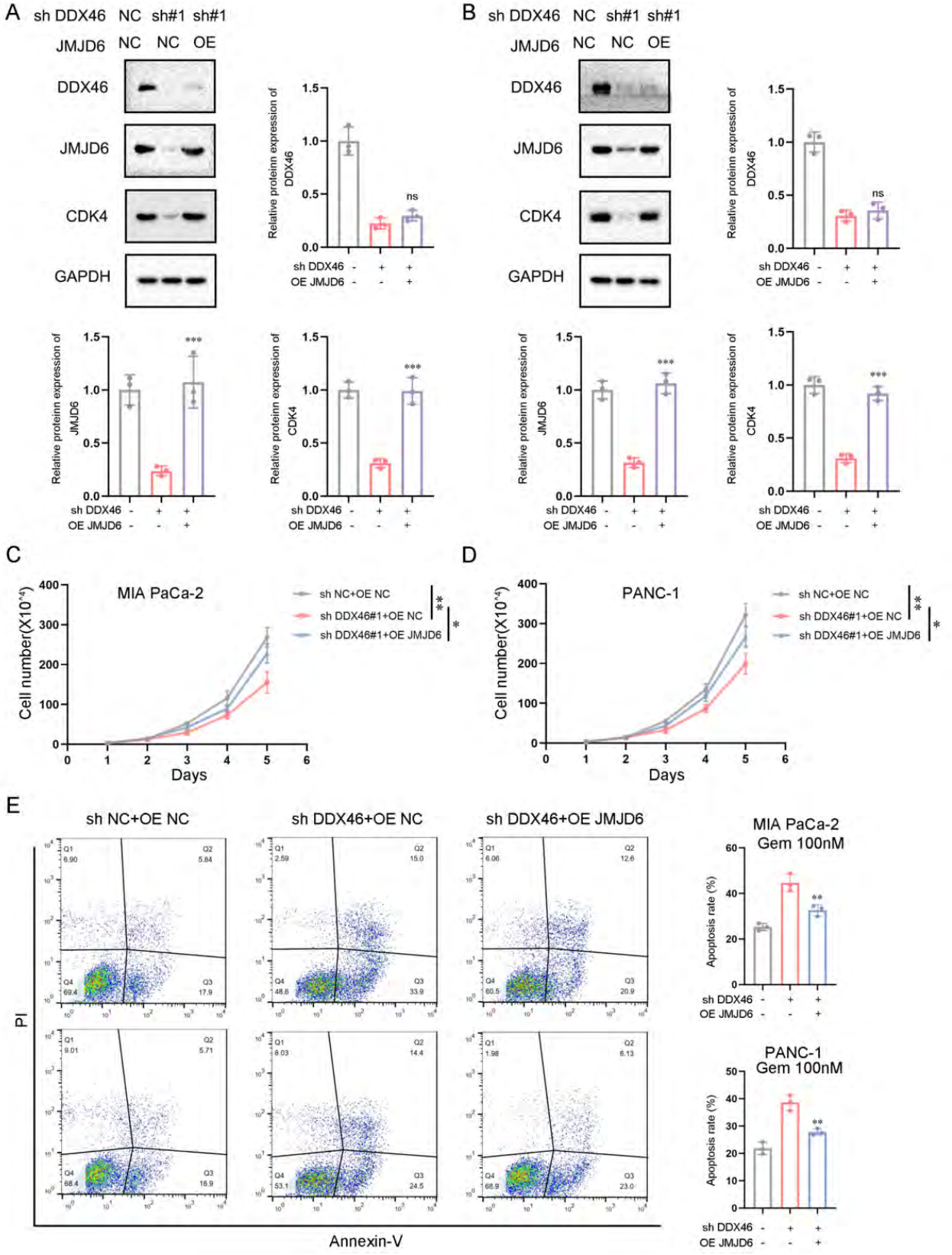

Fig. 7 Download full resolution image